Hydrogel behavior of a sugar-based gelator by introduction of an unsaturated moiety as a hydrophobic group†

Jong Hwa Jung,*[a] Jeong Ah Rim,[b] Won Seok Han,[b] Soo Jin Lee,[a] Young Joo Lee,[b] Eun Jin Cho,[b] Jong Seung Kim,[c] Qingmin Ji[d] and Toshimi Shimizu[d]

Received 15th February 2006, Accepted 20th March 2006
First published as an Advance Article on the web 18th April 2006
DOI: 10.1039/b602279k

The new sugar-based gelators **1** and **2** were synthesized, and their gelation abilities were evaluated in organic solvents and in water. Compound **1** gelates both water and organic solvents whereas **2** gelates only organic solvents. Superstructural difference between hydrogel **1** and organogel **2** was investigated by CD, TEM, AFM, ^{1}H NMR and XRD. Hydrogel **1** displays a well-developed helical ribbon structure with 20–150 nm diameter and a length of several hundred μm whereas organogel **2** shows a twisted fiber structure of diameter 20 nm. CD measurements of hydrogel **1** and organogel **2** indicate that hydrogel **1** maintains a well-ordered chiral structure whereas organogel **2** maintains a relatively disordered chiral structure. The ^{1}H NMR and XRD results suggest that the hydrophobic interaction in hydrogel **1** are relatively weak, with a relatively small region interdigitated between lipophilic alkyl groups. In addition, upon irradiation at 254 nm wavelength, hydrogel **1** reveals a red coloration at 540 nm. These results indicate that the self-assembled hydrogel **1** was polymerized by UV-irradiation. The intensity of the CD spectrum of the polymerized hydrogel markedly decreased. This result indicates that upon polymerization the highly ordered chiral structure of hydrogel **1** changes to a disordered molecular packing structure.

Introduction

A recent issue in supramolecular chemistry is the focus on the organization of monomeric species into desired superstructures. There has been an intense interest in the development of efficient and tunable small molecule gelators for industrial purposes (*e.g.*, in foods, deodorants, cosmetics, athletic shoes and chromatography), as a consequence of versatile gel functions on both microscopic and macroscopic scales.[1–6] Those materials are characterized by more than one length scale, through noncovalent interactions (hydrogen bonding, solvophobic effects, charge transfer and van der Waals interactions). Many organogelators that form hierarchical networks of superstructures in organic fluids have been synthesized. To date, however, only a limited number of "hydrogels" composed of such aggregates have been reported.[2c,7] In this context, most researchers have made hydrogelators by adding various types of hydrophilic group (*e.g.*, peptide, amino acid, ammonium ion or sugar, *etc.*) to gelators.[2c,7] However, corresponding studies of the hydrogelators with unsaturated hydrophobic groups have never been explored to date.

Since most organogelators are rarely soluble in water due to their hydrophobic property, development of a water-soluble hydrogelator based on a sugar-based organogelator applicable for drug delivery systems and medical implants has been our major challenge in this research. Recently, we found that aldopyranose amphiphilic gelators can gelate water in the presence of a small amount of polar organic solvent or of several other organic solvents.[7a,b]

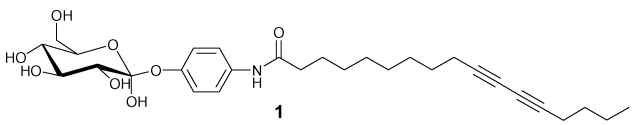

1

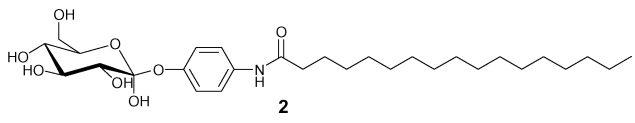

2

In a continuation of our work on the application of organogelators as hydrogelators, we designed and synthesized **1** having a sugar moiety as the hydrophilic group and an unsaturated diacetylene unit as the hydrophobic group. Particularly, the unsaturated alkyl chain group would result in a loose molecular packing structure of the hydrogel formed from **1**. In order to investigate the influence of the unsaturated diacetylene unit on the gelation we also prepared **2**, having saturated hydrocarbons as a reference.

Results and discussion

The gelators **1** and **2** were synthesized as shown in Scheme 1 and their structures were identified by ^{1}H NMR, FT-IR, Mass spectroscopy and elemental analyses (see Experimental Section).

[a]*Department of Chemistry, Research Institute of Natural Science, Gyeongsang National University, Chinju 660-701, S. Korea. E-mail: s_jielee@gaechuk.gsnu.ac.kr; Fax: +82-55-761-0244; Tel: +82-55-751-6021*
[b]*Korea Basic Science Institute (KBSI), Daejeon 305-333, Korea*
[c]*Department of Chemistry, Institute of Nanosensor & Biotechnology, Dankook University, Seoul, 140-714, Korea*
[d]*Nanoarchitectonics Research Center (NARC), National Institute of Advanced Industrial Science and Technology (AIST), Tsukuba Central 5, 1-1-1 Higashi, Tsukuba, Ibaraki 305-8562, Japan*
† Electronic supplementary information (ESI) available: Figures S1 and S2. See DOI: 10.1039/b602279k

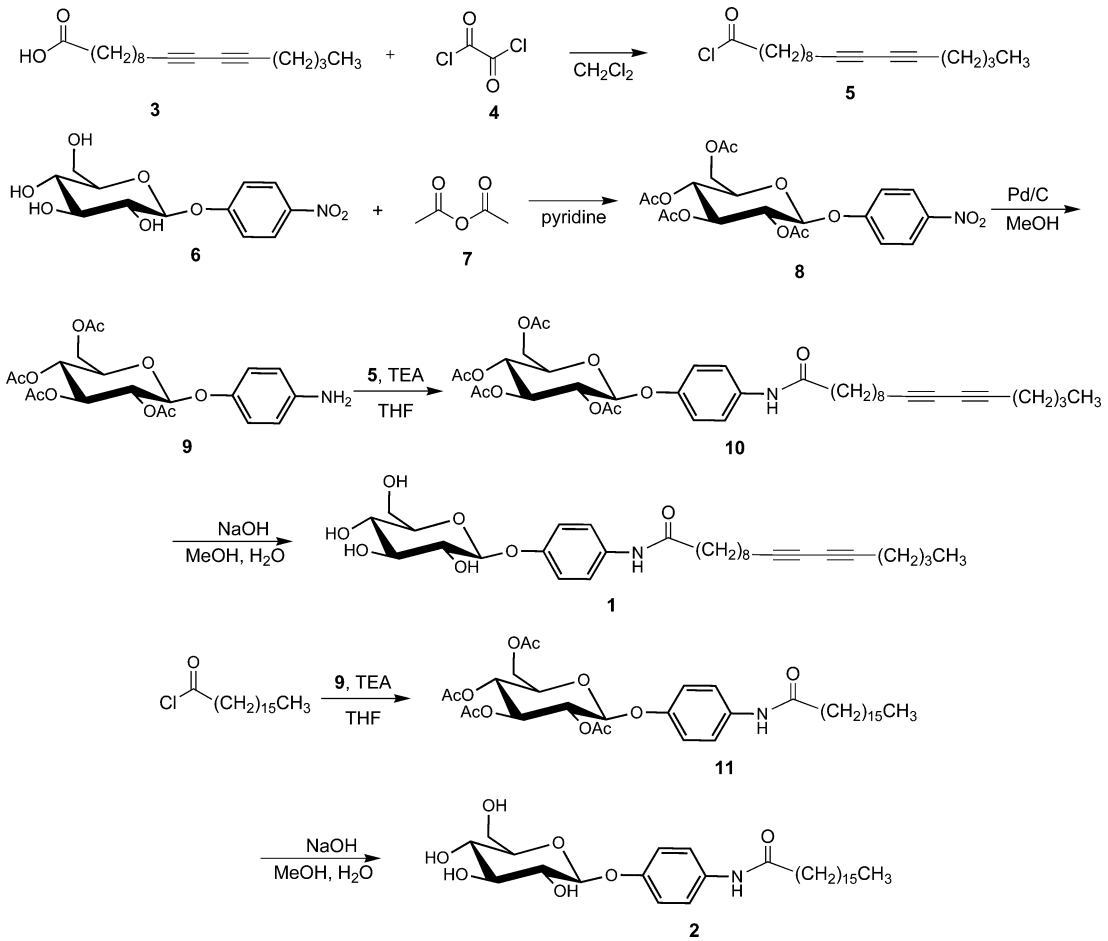

Scheme 1 Synthetic routes for gelators **1** and **2**.

The gelation ability of sugar-based **1** and **2** toward various organic solvents and water was examined by dissolving approximately 0.1–10 mg of compound in 1.0–2.0 mL of the testing solvent followed by heating. Upon cooling to room temperature, a gel, a precipitate, or a clear solution was obtained, depending on the solvents used. The results are summarized in Table 1. Compound **1** showed only 3 'G' with 1 'PG', 1 'I' and 8 'S' whereas **2** gelated 9 among 13 solvents. This observation seems to be much related to solubility of the compounds in the solvents tested. The better solubility in the solvent, the poorer is the gelation ability of the compound.

Table 1 Gelation ability[a] of **1** and **2** in organic solvents and water

Solvent	1	2
Methanol	S	S
Ethanol	S	S
n-Butanol	S	G
tert-Butanol	S	G
Tetrahydrofuran	S	G
Chloroform	G	G
Dichloromethane	G	G
n-Hexane	I	I
Ethyl acetate	PG	G
Dimethylformamide (DMF)	S	G
Dimethyl sulfoxide (DMSO)	S	G
Water	G	I
Water–Methanol (1 : 1 v/v)	S	G

[a] Gelator = 0.05–5.0 wt%. G: stable gel formed at room temperature. S: soluble. I: insoluble. PG: partially gelatinized.

Of particular interest is that in the absence of organic solvents water gelation by gelator **1** was successful, but that by **2** was not. It is noteworthy in this study that the triple bond of **1** plays an important role in the gelation of water. This feature is due to the relatively stronger intermolecular hydrogen-bonding interaction between the sugar moieties of **1** by disordered molecular packing structure between diacetylene moieties, in comparison with the gelator **2**.

Upon irradiation by 254 nm wavelength, gelator **1** reveals a red coloration at 540 nm (Fig. 1A). The intensity of the shifted band increased with time and was maximized upon 32 min irradiation, as shown in Fig. 1A. These results indicate that the self-assembled hydrogel **1** was polymerized by UV-irradiation.

To obtain an insight into the chiral orientation of the gelator in the hydrogel system, we took CD spectra of hydrogel **1** and organogel **2** (Fig. 1B). The λ_{max} values of **1** and **2** in the UV absorption spectra appear at around 225 nm (Electronic Supplementary Information: Fig. S1†) which corresponds to $\lambda_{\theta=0}$ in the CD spectra. The CD spectra of both hydrogel **1** and organogel **2** exhibit a negative first Cotton effect, implying that their dipole moments orient to a clockwise direction in the aggregate of the gels (Fig. 1B). In contrast, no CD Cotton effect was observed

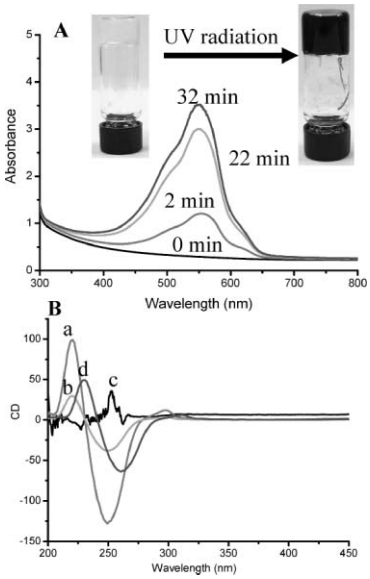

Fig. 1 (A) UV-vis absorption spectra for hydrogel **1** in water [inset, photo images of the self-assembled nanofibers derived from **1** in water (left) and in the polymerized nanofibers with UV irradiation (right)]. (B) CD spectra of hydrogel **1** (a) before and (b) after polymerization, and (c) methanol solution **1** (0.1 wt%). (d) the mixed water–methanol gel **2**.

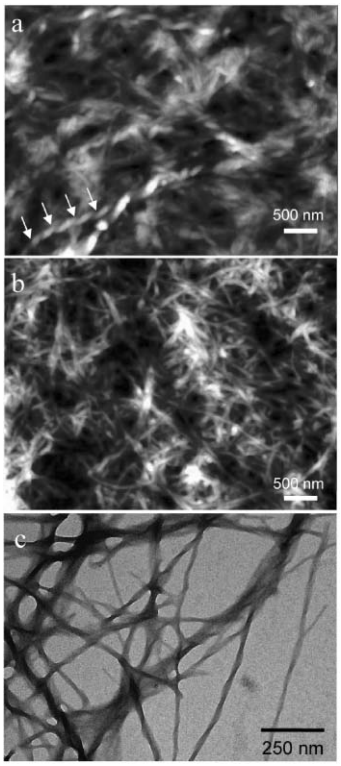

Fig. 2 AFM images of hydrogel **1** (a) before and (b) after polymerization. (c) TEM image of the mixed water–methanol gel **2**.

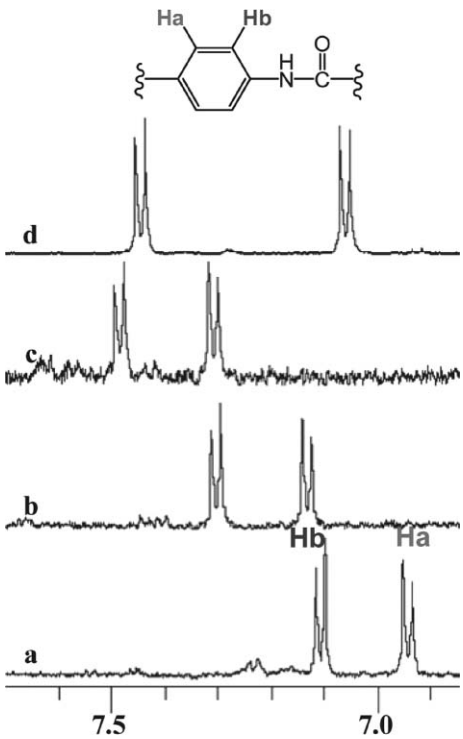

Fig. 3 ^{1}H NMR spectra of hydrogel **1** at (a) 30 °C, (b) 50 °C, (c) 70 °C and (d) CD_3OD solution of **1** at 30 °C.

for **1** in methanol, indicating that the hydrogel forms a highly ordered, chiral structure in comparison to the solution state. In addition, before polymerization, intensity of the CD signal of **1** is much higher than that of hydrogel **2**, suggesting that hydrogel **1** has a highly ordered chiral structure. On the other hand, we observed a markedly decreased CD spectrum of hydrogel **1** when it was polymerized. With this result, we can imagine that upon the polymerization a highly ordered chiral structure of hydrogel **1** changes to a disordered molecular packing structure (*vide-infra*).

To obtain visual insights into the aggregation mode of hydrogel **1** and organogel **2**, we took AFM images of the self-assembled gel **1** before and after polymerization. Before polymerization, hydrogel **1** displays a well-developed helical ribbon structure of diameter 20–150 nm and a length of several hundred μm (Fig. 2a). On the other hand, upon polymerization, **1** revealed a typical fiber structure with a diameter of 20 nm (Fig. 2b), but not a well-defined helical structure, which is in good accordance with our CD observations (*vide supra*). After polymerization, the macroscopic helicity of hydrogel **1** decreased in comparison to that before polymerization. This finding indicates that upon polymerization, the helical molecular packing structure of **1** becomes disordered, which also decreases the macroscopic and microscopic helicities of hydrogel **1**. In contrast, the self-assembled morphology of organogel **2** observed by TEM in the presence of methanol displays a twisted fiber structure with a 30 nm diameter, showing that the macroscopic helicity of organogel **2** is weak in comparison to hydrogel **1**.

In general, NMR techniques can provide a great deal of information on the self-assembly process in the gel state. ^{1}H NMR experiments, especially, may give an insight into how molecules are oriented in the self-assembled state. Aromatic proton signals of hydrogel **1** appeared at 7.12 and 6.90 ppm (Fig. 3a), whereas aromatic proton signals of **1** in CD_3OD solution appeared at 7.43 and 7.06 ppm (Fig. 3d). Upon heating, the aromatic proton signals of the hydrogel **1** are gradually shifted downfield, suggesting that the self-assembled hydrogel **1** forms strong π–π stacking interaction between phenyl groups.

We also observed peak changes in the infra-red spectrum of the gelator **1**. The declining C≡C stretching band at 2254 cm^{-1} by UV-irradiation supports the proposed polymerization of **1** within the nanofibers (See graphical abstract, and ESI: Fig. S2†). The molecular weight of the polymerized nanofiber could not be determined because of its poor solubility in organic solvents such as DMSO, DMF, THF, $CHCl_3$, CH_3OH and toluene.

From X-ray diffraction patterns we also obtained important information for the molecular packing mode of the gelator molecules, as shown in Fig. 4. The X-ray diffraction diagram of hydrogel **1** before polymerization reveals a single sharp peak at $d = 4.05$ nm in the small-angle region (Fig. 4A). This length of 4.05 nm is shorter than twice that of the extended molecular length of **1** (2.9 nm, by CPK molecular modeling), but longer than the length of one molecule. Thus, the hydrogel **1** should have an interdigitated bilayer structure with a thickness of 4.05 nm (Fig. 4A-a and Fig. 4B-a). On the other hand, the obtained long spacing (d) of hydrogel **1** upon the polymerization was 4.20 nm, slightly larger than that before polymerization (Fig. 4A-b and Fig. 4B-b). This might be due to a loose chiral packing structure between sugar moieties resulting from the polymerization.

The obtained long spacing (d) of organogel **2** was 3.70 nm (one molecular length = 3.2 nm). This value is also compatible with a bilayer structure with a relative large region interdigitated by hydrophobic interactions, forming a relatively stronger hydrophobic interaction. Thus one can suggest that the hydrogel **1** forms a bilayer structure with a relatively small region interdigitated through hydrophobic interactions, unlike organogel **2**.

Conclusions

We demonstrated that the sugar-based gelator **1** containing a lipophilic diacetylene group can gelate water efficiently in the absence of organic solvent even at extremely low concentration (0.05 wt%). The hydrogel **1** forms a well-ordered bilayer structure in water by self-assembly through intermolecular hydrogen bonding, π–π stacking and interdigitated hydrophobic interactions, in contrast to the sugar-based gelator **2**. In addition, upon irradiation at a wavelength of 254 nm, the hydrogel **1** reveals a red coloration at 540 nm. These results indicate that the self-assembled hydorgel **1** was polymerized by UV-irradiation. The intensity of the CD spectrum of the hydrogel was markedly decreased following polymerization. This finding indicates that upon polymerization the highly ordered chiral structure of hydrogel **1** changes to a disordered molecular packing structure. Consequently, the hydrogelator could be an innovative tool in drug delivery systems and medical implants.

Experimental

Spectroscopy measurements

^1H and ^{13}C NMR spectra were measured on a Bruker ARX 300 apparatus. IR spectra were obtained in KBr pellets using a Shimadzu FT-IR 8100 spectrometer, and MS spectra were obtained with a Hitachi M-250 mass spectrometer. Circular dichroism (CD) spectra were measured on a JASCO J-820KS spectrophotometer (cell diameter 10 mm).

XRD measurements

The XRD of a freeze-dried sample was measured with a Rigaku diffractometer (Type 4037) using graded d-space elliptical side-by-side multilayer optics, monochromated Cu K_α radiation (40 kV, 30 mA), and an imaging plate (R-Axis IV). The typical exposure time was 10 min with a 150 mm camera length. Freeze-dried samples from **2**–**9** were vacuum-dried to constant weight and then put into capillary tubes, without being powdered.

TEM observations

The aqueous dispersions of the nanostructures (0.1 mg mL^{-1}) were dripped onto an amorphous carbon grid, and excess water was blotted with filter paper. TEM was done with a Carl-Zeiss LEO912 instrument operated at 50 keV. Images were recorded on an imaging plate (Fuji Photo Film Co. Ltd. FDL5000 system) with 20 eV energy windows at 3000–250 000 × and were digitally enlarged.

Gelation test of organic fluids

In typical gelation experiment, a weighed amount of gelator and 0.1–1 mL of the solvent were put in a sample bottle, after which the

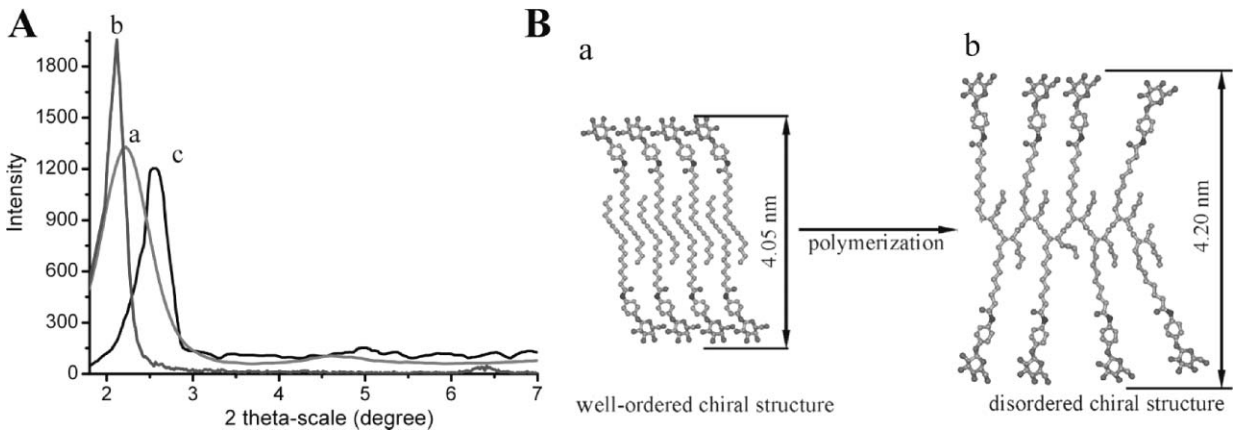

Fig. 4 (A) Power-XRD patterns of hydrogel **1** (a) before and (b) after polymerization and (c) mixed water-methanol gel **2**. (B) Proposed molecular packing modes of hydrogel **1** (a) before and (b) after polymerization.

sample bottle was tightly sealed with a screw cap. The bottle was then heated with shaking until all the solid material had dissolved. The solution was set aside and allowed to cool to 25 °C. Gelation was stable to inversion when the sample bottle was turned upside down.

Synthesis

Compounds **3**, **4**, **6** and **7** are commercially available.

***N*-(4-((2*S*,3*S*,4*S*,5*S*)-3,4,5-Trihydroxy-6-(hydroxymethyl)-tetrahydro-2*H*-pyran-2-yloxy)phenyl) heptadeca-10,12-diynamide (1).** A mixture of **9** (0.15 g, 0.33 mmol) and NaOH (0.52 g, 1.3 mmol) in MeOH (16 mL) and H_2O (4 mL) was stirred for 3 h at room temperature. The solution was concentrated *in vacuo*, and acidified with 0.1 M HCl solution. The precipitate was filtered and dried *in vacuo.* White solid. Mp: 123–126 °C. Yield 90%. ^{1}H NMR (300 MHz, DMSO-d_6): δ 9.70 (s, 1H, N*H*), 7.49 (d, 2H, J = 9, Ar–*H*), 6.97 (d, 2H, J = 9, Ar–*H*), 5.24 (d, 1H), 5.24 (d, 1H), 5.02 (d, 1H), 4.96 (d, 1H), 4.77(d, 1H), 4.52(t, 1H), 3.72 (m, 1H), 3.48 (m, 1H), 3.26(s, 5H), 2.30 (m, 6H), 1.57 (m, 2H), 1.45–1.28 (m, 14H), 0.89 (t, 3H, C*H*$_3$); ^{13}C NMR (75 MHz, $CDCl_3$): 181.3, 148.4, 125.1, 118.8, 115.3, 85.3, 74.5, 70.6, 65.8, 64.6, 63.1, 25–28, 20.5, 13.1 ppm; IR (KBr, cm^{-1}): 3378, 3288, 2929, 2850, 1654, 1604, 1533, 1509, 1407, 1234, 1074; MS (FAB): 544 (M + H)$^+$ (calcd MW = 543.3); elemental analysis: calcd (%) for $C_{31}H_{45}NO_7$: C 68.10, H 8.44, N 2.54; found: C 68.48, H 8.34, N 2.58.

***N*-(4-((2*S*,3*S*,4*S*,5*S*)-3,4,5-Trihydroxy-6-(hydroxymethyl)-tetrahydro-2*H*-pyran-2-yloxy)phenyl)heptadecanamide (2).** Synthetic procedures are same as for **1** starting from **11**. ^{1}H NMR (300 MHz, DMSO-D_6): δ 9.60 (s, 1H, N*H*), 7.50 (d, 2H, J = 9, Ar–*H*), 6.88 (d, 2H, J = 9, Ar–*H*), 5.13 (d, 1H), 5.20 (d, 1H), 4.99 (d, 1H), 4.88 (d, 1H), 4.70(d, 1H), 4.61(t, 1H), 3.80 (m, 1H), 3.18(s, 5H), 1.50 (m, 2H), 1.45–1.28 (m, 30H), 0.82 (m, 3H, C*H*$_3$); ^{13}C NMR (75 MHz, $CDCl_3$): 171, 131.0, 121.5, 116.2, 102.2, 71.1, 66.0, 65.7, 65.2, 64.2, 31–27, 21.5, 12.5 ppm; IR (KBr, cm^{-1}): 3375, 3288, 2929, 2850, 1654, 1600, 1535, 1512, 1407, 1234, 1072; MS (FAB): 538.5 (M + H)$^+$ (calcd MW = 537.73); elemental analysis: calcd (%) for $C_{30}H_{51}NO_7$; C 67.01, H 9.56, N 2.60. found: C 65.07, H 9.11, N 2.50.

10, 12-Heptadecadiynoyl chloride (5). A mixture of 10,12-heptadecadiynoic acid **3** (0.10 g, 0.37 mmol), **4** (0.12 mL, 3.96 mmol) and DMF (1 ~ 2 drops) was dissolved in CH_2Cl_2 (2.0 mL), and the reaction mixture was then stirred for 10 h at room temperature. The residual oxalyl chloride and solvent were removed *in vacuo.* The product was directly used for the coupling reaction without further purification.

(2*R*,3*R*,4*S*,5*R*,6*S*)-2-(Acetoxymethyl)-6-(4-nitrophenoxy)-tetrahydro-2*H*-pyran-3,4,5-triyl triacetate (8). Nitrophenyl-β-D-glucopyranoside **6** (1.0 g, 2.54 mmol) was dissolved in 1.0 mL of pyridine and 1.0 mL of **7**. The reaction mixture was allowed to stand overnight and was then evaporated *in vacuo* to dryness with dry toluene. The residue was purified by column chromatography on silica gel with EA/Hx (1/1 v/v, R_f = 0.5). Yield 75%. ^{1}H NMR (300 MHz, $CDCl_3$): δ 7.23 (d, 2H, J = 9, Ar–*H*), 7.08 (d, 2H, J = 9, Ar–*H*), 5.24 (m, 3H), 5.04 (d, 1H, J = 9), 4.3–4.1 (m, 2H), 3.87 (m, 1H), 1.97 (s, 12H); ^{13}C NMR (75 MHz, $CDCl_3$): 170.5, 158.6, 130.5, 123.1, 115.3, 98.1, 71.4, 68.3, 65.4, 20.8, 19.6 ppm; MS (FAB): 470 (M + H)$^+$ (calcd MW = 469.1); elemental analysis calcd (%) for $C_{20}H_{23}NO_{12}$: C 51.18, H 4.94, N 2.98; found: C 51.01, H 5.24, N 2.86.

(2*R*,3*R*,4*S*,5*R*,6*S*)-2-(Acetoxymethyl)-6-(4-aminophenoxy)-tetrahydro-2*H*-pyran-3,4,5-triyl triacetate (9). Compound **8** (1.0 g) was dissolved with 25 mL of MeOH. After 5 min of N_2 purging, Pd on activated carbon (10 wt%, 100 mg) was added. Under 2 atm of H_2, the reaction was allowed to proceed for 3 h. After filtration and evaporation, pure **9** was obtained as a pale yellow solid (2.48 g, quantitative). (1/1 v/v, R_f = 0.5). Yield 75%. ^{1}H NMR (300 MHz, $CDCl_3$, 25 °C): δ 6.85 (d, 2H, J = 9, Ar–*H*), 6.64 (d, 2H, J = 9, Ar–*H*), 5.24 (m, 3H), 4.96 (d, 1H, J = 9), 4.3–4.1 (m, 2H), 3.81 (m, 1H), 3.48 (s, 2H), 2.05 (s, 12H); ^{13}C NMR (75 MHz, $CDCl_3$): 170.3, 158.9, 130.2, 121.0, 119.3, 97.1, 73.4, 69.1, 64.6, 20.5, 19.1 ppm; MS (FAB): 438 (M + H)$^+$ (calcd MW = 439.1); elemental analysis: calcd (%) for $C_{20}H_{25}NO_{10}$: C 54.89, H 6.10, N 3.40; found: C 54.67, H 5.73, N 3.19.

(3*R*,4*S*,5*S*,6*S*)-2-(Acetoxymethyl)-6-(4-heptadeca-10,12-diynamidophenoxy)-tetrahydro-2*H*-pyran-3,4,5-triyl triacetate (10). A mixture of **5** (0.15 g, 0.34 mmol), **9** (0.1 g, 0.34 mmol), and triethylamine (0.17 g, 1.7 mmol) in dry THF (20 mL) was refluxed for 3 h under N_2 atmosphere. The solution was filtered after cooling to room temperature, and concentrated *in vacuo.* The residue was purified by column chromatography on silica gel with EA/Hx (2/1 v/v, R_f = 0.6). Yield 75%. ^{1}H NMR (300 MHz, $CDCl_3$): δ 9.70 (s, 1H, N*H*), 7.49 (d, 2H, J = 9, Ar–*H*), 6.97 (d, 2H, J = 9, Ar–*H*), 5.21 (d, 1H), 5.16 (d, 1H), 4.98 (d, 1H), 4.91 (d, 1H), 4.75(d, 1H), 4.58(t, 1H), 3.78 (m, 1H), 3.35 (m, 1H), 3.21(s, 5H), 2.33 (m, 6H), 2.08 (m, 12H), 1.53 (m, 2H), 1.45–1.28 (m, 14H), 0.83 (s, 3H, C*H*$_3$); ^{13}C NMR (75 MHz, $CDCl_3$): 180.2, 169.3, 155.4, 129.1, 119.9, 119.1, 89.1, 77.4, 71.3, 69.1, 64.6, 61.1, 25–28, 20.5, 19.1, 12.8 ppm; MS (FAB): 713 (M + H)$^+$ (calcd MW = 711.4); elemental analysis calcd (%) for $C_{39}H_{53}NO_{11}$: C 65.14, H 8.21, N 2.01; found: C 65.80, H 7.50, N 1.97.

(3*R*,4*S*,5*S*,6*S*)-2-(Acetoxymethyl)-6-(4-heptadecanamidophenoxy)-tetrahydro-2*H*-pyran-3,4,5-triyl triacetate (11). The same reaction procedures as for **10** were used starting from stearoyl chloride and **9**. ^{1}H NMR (300 MHz, CDCl): δ 9.70 (s, 1H, N*H*), 7.49 (d, 2H, J = 9, Ar–*H*), 6.97 (d, 2H, J = 9, Ar–*H*), 5.21 (d, 1H), 5.16 (d, 1H), 4.98 (d, 1H), 4.91 (d, 1H), 4.75(d, 1H), 4.58(t, 1H), 3.78 (m, 1H), 2.08 (m, 12H), 1.53 (m, 2H), 1.45–1.28 (m, 30H), 0.82 (m, 3H, C*H*$_3$); ^{13}C NMR (75 MHz, $CDCl_3$): 178, 171.2, 156.2, 128.6, 121.4, 110.6, 97.1, 75.0, 73.1, 66.1, 65.1, 64.1, 33–27, 20.8, 16.1; MS (FAB): 706.5 (M + H)$^+$ (calcd MW = 705.41); elemental analysis: calcd (%) for $C_{38}H_{59}NO_{11}$: C 64.66, H 8.42, N 1.98.; found: C 64.35, H 8.22, N 2.00.

Acknowledgements

This work was supported by the KOSEF (F01-2004-10061-0 and R01-2005-000-10229-0).

References

1 For recent comprehensive reviews, see: (*a*) E. Otsuni, P. Kamaras and R. G. Weiss, *Angew. Chem., Int. Ed. Engl.*, 1996, **35**, 1324; (*b*) P. Terech and R. G. Weiss, *Chem. Rev.*, 1997, **97**, 3133; (*c*) J. H. van Esch and

B. L. Feringa, *Angew. Chem., Int. Ed.*, 2000, **39**, 2263; (*d*) D. J. Abdallah and R. G. Weiss, *Adv. Mater.*, 2000, **12**, 1237.
2 (*a*) K. Hanabusa, T. Miki, Y. Taguchi, T. Koyama and H. J. Shirai, *J. Chem. Soc., Chem. Commun.*, 1993, 1382; (*b*) K. Hanabusa, M. Yamada and H. Shirai, *Angew. Chem., Int. Ed. Engl.*, 1996, **35**, 1949; (*c*) M. Suzuki, M. Yumoto, M. Kimura, H. Shirai and K. Hanabusa, *Chem.–Eur. J.*, 2003, **9**, 348.
3 (*a*) M. Loos, J. Esch, I. Stokroos, R. M. Kellogg and B. L. Feringa, *J. Am. Chem. Soc.*, 1997, **119**, 12675; (*b*) J. van Esch, S. De Feyter, R. M. Kellogg, F. De Schryver and B. L. Feringa, *Chem.–Eur. J.*, 1997, **3**, 1238; (*c*) S. van der Laan, B. L. Feringa, R. M. Kellogg and J. van Esch, *Langmuir*, 2002, **18**, 7136; (*d*) R. J. H. Hafkamp, P. A. Kokke, I. M. Danke, H. P. M. Guerts, A. E. Rowan, M. C. Feiters and R. J. M. Nolte, *Chem. Commun.*, 1997, 545; (*e*) R. J. H. Hafkamp, M. C. Feiters and R. J. M. Nolte, *J. Org. Chem.*, 1999, **64**, 412.
4 (*a*) R. Wang, C. Geiger, L. Chen and D. G. Whitten, *J. Am. Chem. Soc.*, 2000, **122**, 2399; (*b*) D. C. Duncan and D. G. Whitten, *Langmuir*, 2000, **16**, 6445; (*c*) C. Geiger, M. Stanescu, L. Chen and D. G. Whitten, *Langmuir*, 1999, **15**, 2241.
5 (*a*) K. Murata, M. Aoki, T. Suzuki, T. Harada, K. Kawabata, T. Komori, F. Ohseto, K. Ueda and S. Shinkai, *J. Am. Chem. Soc.*, 1994, **116**, 6664; (*b*) K. Yoza, N. Amanokura, Y. Ono, T. Akao, H. Shinmori, M. Takeuchi, S. Shinkai and D. N. Reinhoudt, *Chem.–Eur. J.*, 1999, **5**, 2722.
6 (*a*) F. M. Menger and K. L. Caran, *J. Am. Chem. Soc.*, 2000, **122**, 11679; (*b*) L. A. Estroff and A. D. Hamilton, *Angew. Chem., Int. Ed.*, 2000, **39**, 3447; (*c*) G. Wang and A. D. Hamilton, *Chem.–Eur. J.*, 2002, **8**, 1954; (*d*) A. Ajayaghosh and S. J. George, *J. Am. Chem. Soc.*, 2001, **123**, 5148; (*e*) M. George and R. G. Weiss, *J. Am. Chem. Soc.*, 2001, **123**, 10393; (*f*) R. Oda, I. Huc and S. J. Candau, *Angew. Chem., Int. Ed.*, 1998, **37**, 2689.
7 (*a*) J. H. Jung, G. John, M. Masuda, K. Yoshida, S. Shinkai and T. Shimizu, *Langmuir*, 2001, **17**, 7229; (*b*) J. H. Jung, S. Shinkai and T. Shimizu, *Chem.–Eur. J.*, 2002, **8**, 2684; (*c*) S. Kiyonaka, S. Shinkai and I. Hamachi, *Chem.–Eur. J.*, 2003, **9**, 976; (*d*) G. Wang and A. D. Hamiton, *Chem. Commun.*, 2003, 310; (*e*) K. J. C. van Bommel, C. van der Pol, I. Muizebelt, A. Friggeri, A. Heeres, A. Meetsma, B. L. Feringa and J. van Esch, *Angew. Chem., Int. Ed.*, 2004, **43**, 1663; (*f*) R. Karinaga, Y. Jeong, S. Shinkai, K. Kaneko and K. Sakurai, *Langmuir*, 2005, **21**, 9398.

